Immune Digital Twin Blueprint: A Comprehensive Simulatable Model of the Human Immune System

Robert Moore[1], Rada Amin[1], Sara Aghamiri[1], Akram Mohammed[2], Alyssa La Fleur[1], Bhanwar Lal Puniya[1], Tomáš Helikar[1]*

Affiliations:
[1]Department of Biochemistry, University of Nebraska-Lincoln, NE
[2]The University of Tennessee Health Science Center

***To whom correspondence should be addressed:**
Tomáš Helikar, Ph.D., Department of Biochemistry, University of Nebraska-Lincoln, USA, Email: thelikar2@unl.edu

Abstract

The immune system is a complex and dynamic network that plays a crucial role in maintaining health and combating infections. Developing an accurate and comprehensive digital twin of the immune system requires a solid foundation that incorporates the essential cellular components and their interactions. In this study, we present the first blueprint for an immune system digital twin, consisting of a comprehensive map and a simulatable logical model. This blueprint integrates 27 innate and adaptive immune cells, 31 cytokines and immunoglobulins, and 9 different pathogens, providing a foundation for developing a multi-scale model. We validate the cellular-level logical model against available experimental data and demonstrate its potential in characterizing system-wide immune responses to various coinfections. By making the model available in easy-to-use formats directly in Cell Collective and as an SBGN map, it can be easily further expanded by the community. This cellular-level blueprint represents a significant step towards the development of general-purpose immune digital twins, with far-reaching implications for the future of digital twin technology in life sciences and healthcare, advancing patient care and accelerating the transition toward precision medicine.

Introduction

Digital twin technology has emerged as a powerful tool for creating virtual representations of real-world systems, allowing for the simulation, analysis, and optimization of these systems in a controlled environment. By generating a digital replica of a physical asset, process, or system, digital twin technology enables engineers, scientists, and decision-makers to anticipate problems, design innovative solutions, and assess the viability of new products before their physical implementation[1,2]. The use of digital twins has grown exponentially across various industries, including manufacturing, automotive, and medical devices, due to their potential to improve efficiency, reduce costs, and minimize risks associated with changes to existing operations or the development of new products[3–5]. As real-world data continually informs the digital twin, the accuracy with which it represents the actual system increases, allowing for more informed decision-making and better predictions of system behavior.

Much of the massive influx of data produced by high-throughput technologies in the biomedical domain consists of discrete snapshots of biological processes, offering an incomplete view of working systems. The life sciences will thus benefit greatly from digital twins that can integrate diverse data sources and reconstruct comprehensive, dynamic models of biological systems to facilitate drug discovery, optimize treatment plans, and even replace traditional clinical trials with simulations on virtual patients. Digital twins provide researchers and healthcare professionals with a deeper understanding of the functions and dysfunctions of complex biological systems, ultimately leading to improved patient outcomes and precision medicine[6,7].

For example, digital twins have been designed to simulate the progression of individual tumors and personalized cancer scenarios, incorporating parameters like magnetic resonance imaging (MRI) data, the intricacies of the tumor microenvironment, genetic alterations, a spectrum of omics data, and responses to treatments [8–10]. These models can be used to predict tumor progression, optimize treatment strategies, and identify potential therapeutic targets.[11–14] Digital twins simulating the function of the human heart and its response to various interventions, such as pacemaker settings or drug therapies, and patient-specific digital twins of vascular systems simulating blood flow, pressure, and other hemodynamic parameters can be used to optimize treatment strategies and predict patient outcomes in heart failure, arrhythmias, and other cardiovascular conditions.[15–17] Digital twins have also been developed for patients with type 1 and type 2 diabetes to simulate glucose metabolism, insulin sensitivity, and the effects of various interventions, such as insulin administration and lifestyle modifications, helping optimize glucose control and personalize diabetes management strategies. [18–21]

The human immune system is an ideal candidate for digital twin development due to its broad medical significance and complexity [22]. Spanning every level of biological organization, the immune system plays a crucial role in many health conditions, including autoimmune diseases, primary immune disorders, allergies, infections, and systemic biological responses related to chronic diseases, wound healing, and trauma. The immune system is a highly complex and dynamic network involving many cellular and molecular components, such as immune cells, cytokines, and immunoglobulins, which interact in a tightly regulated manner. An accurate understanding of the system requires integrating these components and their interactions into a coherent and consistent model.

This manuscript introduces a comprehensive map and a simulatable (logical) model of the immune system as the first blueprint of an immune system digital twin - a key initial step towards the development of an immune digital twin recently identified by the community [22]:

<u>Establishing a foundation</u>: The immune system spans different temporal scales and levels of biological organization, including molecular, cellular, tissue, organ, and organism levels. The blueprint provides a solid foundation for a multi-scale model, ensuring that the essential cellular components and their interactions are accurately represented before introducing other levels of biological organization. [22]

<u>Guiding model development</u>: The blueprint serves as a guide for constructing the multi-scale model, helping researchers identify critical components and interactions that need to be

integrated across different scales and ensuring that the model remains consistent and coherent as it expands to encompass additional levels of biological complexity. [22]

Facilitating validation and refinement: Having a well-defined blueprint allows the community to validate and refine the model more effectively, comparing its predictions with experimental data at different levels of biological organization and making necessary adjustments to improve its accuracy and reliability.

Enhancing collaboration and interdisciplinary research: A comprehensive blueprint of the immune system can facilitate collaboration among researchers from different disciplines, providing a common framework and language to understand the immune system's complexity and interactions.

Methods

Systems Biology Graphical Notation (SBGN) map construction

We constructed a Systems Biology Graphical Notation (SBGN) Activity Flow map of the immune digital twin (IDT) blueprint to illustrate the functional relationships between the various entities of the model. SBGN provides a set of standardized and coherent visual languages to represent biological pathways [23]. In the Activity Flow language, nodes represent the biological activities of cells and molecules, and edges represent influences between them, such as stimulation and inhibition. We created the map with CellDesigner [24], a structured editor. We named molecular activities with the HGNC symbol [25] of the gene coding for the protein carrying the activity. To streamline the flow of information, we organized the SBGN map into five distinct layers: pathogens, non-immune target cells, innate immune cells, adaptive immune cells, and secreted molecules. The map is encoded in the CellDesigner annotations of an SBML Level 3.[26] To visualize the map, we used the Minerva platform[27], enabling seamless navigation through various zoom levels.

Model construction and mathematical framework

We chose logical modeling to represent the cellular-level interactions within the immune system accurately in the absence of comprehensive quantitative kinetic information. Logical models use rules to describe the relationships between various components of a biological system, such as activation, inhibition, and feedback loops [28–31]. We represented each immune cell type, cytokine, immunoglobulin, and pathogen as a distinct component, with edges illustrating their interactions. The components are assigned discrete values (e.g., 0 for inactive and 1 for active) based on the presence or absence of a specific component's activity, while logical rules dictate the state transitions between these values. We built and curated the model in the web-based modeling and analysis platform Cell Collective. [32] All components and individual interactions used to build the regulatory mechanisms have been annotated in Cell Collective with the exact quote from the reference literature. The model is publicly available in Cell Collective, where it can be simulated,

further expanded, and downloaded in several file formats (such as SBML-qual [33,34], text files containing the logical functions, and truth tables).

Model simulations and analyses

We used Cell Collective for all computational simulations and analyses. This platform utilizes discrete mathematics to construct the model, while the simulated output values exhibit semi-continuous behavior, spanning from 0 to 100% activity levels. [30,32] External components' activity levels are dimensionless and represent a percentage chance that a component is active at a specific time *t*. It is important to note that the activity levels provide a semi-quantitative measure of the relative activity of a particular component rather than a specific biological measurement (e.g., concentration). Users can tailor external components' activity levels as required by the simulation experiment, either by setting specific values or by defining a range from which values are randomly sampled before each simulation (e.g., for simulating dose-response experiments).

We conducted two types of analyses: real-time and dose-response. These analyses used asynchronous updates, allowing the transition times, i.e., the change of activity for cells and gene products, to reflect more accurately biological phenomena.

Each experiment simulating a single infection consisted of 1000 simulations with different randomly sampled external component activity levels (within 0–100 %). The simulations were asynchronous and lasted 800 steps. Output components' activity levels were calculated as the fraction of 0's and 1's over the last 300 iterations [30,35,36]. As noted previously [30,36] and from observations drawn from the model presented here (data not shown), the model reaches steady-state rapidly, and these values are sufficient to describe the network's "long-term" (e.g., attractor-like) behavior.

To simulate sequential coinfection, we adopted a three-stage approach: (1) step 1 to step 99 were run without any infection, (2) at step 100, we added the first pathogen, and (3) at step 500, we added the second pathogen. We collected the data from steps 300 to 150. We ran 1000 simulations for each pair of infections. We performed perturbation analyses to evaluate which components' knockout or overexpression led to significant variations in the network dynamics. A knockout implies the deactivation of a component during an entire simulation, whereas an overexpression generates the permanent activation of a component.

Simulation settings

Each pathogen is represented by an external component (independent variable) in the model whose activity level can be set by the user. Each immune cell also possesses an associated external component so that its initial levels can be set to represent different immune system health statuses for different conditions or sub-populations. For single infections, we used four different ranges of pathogen activity levels (i.e., viral load), low (5-15%), medium (45-55%), high (85-95%), and all (0-100%), representing the severity of infection. For coinfections, both pathogens were simulated under high viral loads at activity levels of 85-95%.

Results

A. Model design and scope

Our comprehensive model captures the intricate network of signals and responses that drive the immune system's defense against infections and comprises 164 variables representing 27 cell types and their various states, 36 molecules, 9 pathogens, and 506 regulatory interactions among these components (Figure 1, Table 1).

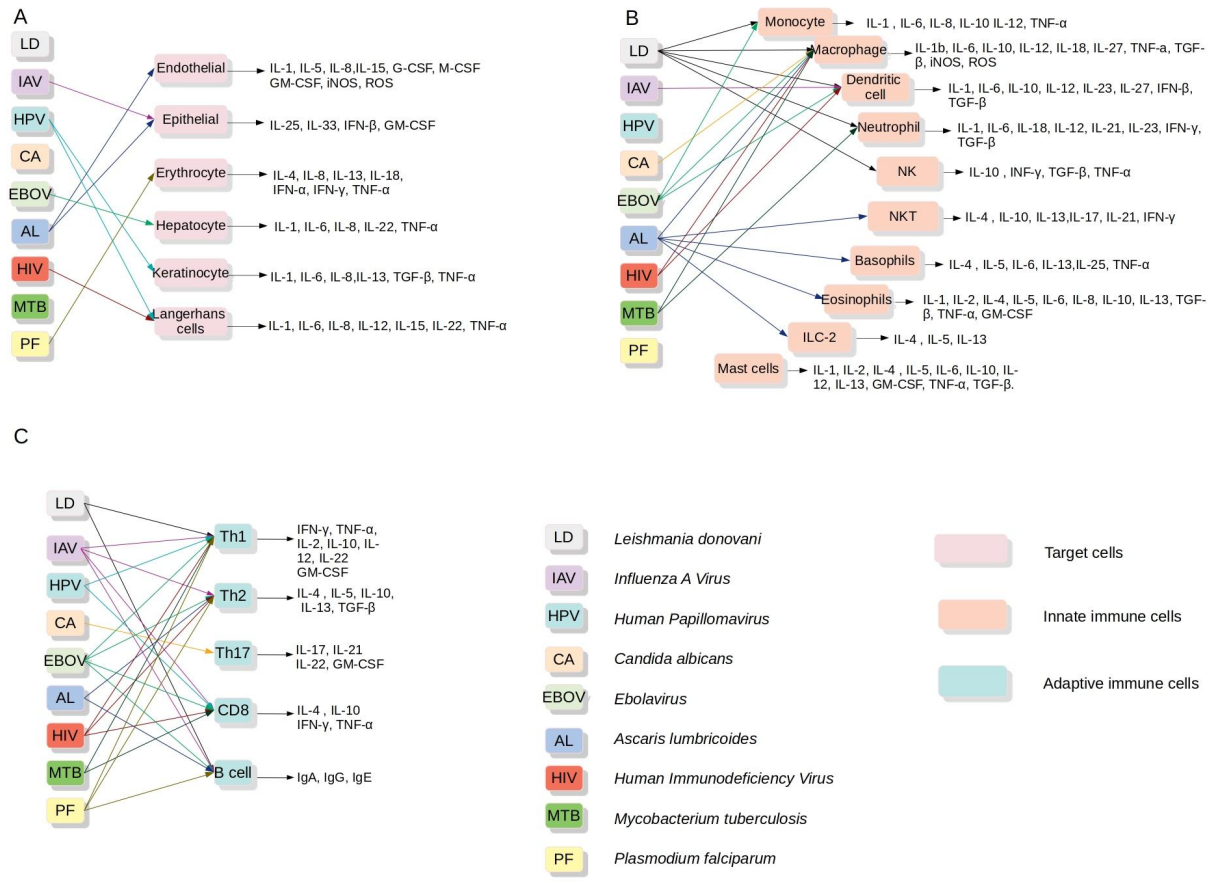

Figure 1: Components of the immune system model. (A) pathogens, non-immune target cells, and secreted cytokines (B) pathogens, innate immune target cells, and secreted cytokines, (C) pathogens, adaptive immune cells, and secreted cytokines and immunoglobulins. In panels A, B, and C, the arrows connecting pathogens to cell types represent stimulation, while the arrows connecting cell types and cytokines represent secretion

Table 1: List of cell types included in the modeled immune system.

Cell Type	Brief Synopsis	Citations
	Innate Immunity	

Basophils	These granulocytes contribute to allergic reactions and inflammation. They are activated when allergens cross-link IgE bound to their FcεRI receptors37. Upon activation, they release histamine and other inflammatory mediators, including IL-4, IL-13, and IL-33, that increase vascular permeability and attract other immune cells, such as eosinophils, to the site of inflammation.	38
Dendritic cells	These antigen-presenting cells form a bridge between the innate and adaptive immune systems. They capture and process antigens, then present them to T cells via MHC molecules, triggering adaptive immune responses. Dendritic cells are activated by PAMPs or DAMPs through PRRs, such as Toll-like receptors. They produce various cytokines, such as IL-12, IL-6, and IL-1, that stimulate T cell differentiation and activation.	39,40
Endothelial cells	These cells line blood vessels and regulate leukocyte adhesion, migration, and blood vessel permeability. Endothelial cells express adhesion molecules (e.g., selectins and integrins) and secrete chemokines, such as IL-8 and MIP-1 alpha, that recruit immune cells, such as neutrophils and monocytes, to sites of inflammation.	41,42
Eosinophils	These granulocytes defend against parasitic infections and contribute to allergic inflammation. Eosinophils are activated by cytokines produced by Th2 cells, such as IL-5, and by other inflammatory mediators, such as leukotrienes. Upon activation, they release cytotoxic granules containing reactive oxygen species (ROS) and release cytokines, such as IL-4, that modulate other immune cell functions.	43
Epithelial cells	These barrier-forming cells are essential for maintaining tissue integrity and preventing pathogen entry. They secrete cytokines, chemokines, and growth factors, such as IL-1, IL-6, IL-8, TGF-β, GM-CSF, and G-CSF, that recruit and activate immune cells, such as neutrophils, macrophages, and dendritic cells.	44
Hepatocytes	These liver cells perform various metabolic functions, including detoxification and synthesis of immune-related proteins, such as acute-phase proteins and complement factors. They can also produce cytokines, such as IL-6, and growth factors, such as M-CSFs, that modulate immune cell activation and differentiation.	45
Group 2 innate lymphoid cells (ILC2)	These cells defend against helminth infections and contribute to allergic inflammation. ILC2s produce type 2 cytokines, such as IL-5 and IL-13, upon activation by epithelial cell-derived cytokines, such as IL-25 and IL-33. They promote eosinophil recruitment and activation, mucus production, and tissue repair.	46
Keratinocytes	These skin cells form part of the physical barrier and produce antimicrobial peptides and cytokines upon activation by PAMPs, DAMPs, or cytokines from other immune cells. They contribute to the recruitment and activation of other immune cells, such as dendritic and Langerhans cells, and reinforce barrier function. Keratinocytes produce cytokines and chemokines, such as IL-1, IL-6, TNF-α, and IL-8, that attract and activate immune cells, such as neutrophils, macrophages, and dendritic cells.	47,48

Langerhans cells	These specialized dendritic cells reside in the skin and mucosal tissues. They capture and process antigens, then migrate to lymph nodes, where they present the antigens to T cells, initiating adaptive immune responses. Langerhans cells produce cytokines, such as IL-12 and IL-23, that stimulate T-cell differentiation and activation.	49
Macrophages	These phagocytic cells engulf and destroy pathogens, remove cellular debris, and produce cytokines that regulate inflammation and immune responses. Macrophages can be activated by PAMPs, DAMPs, or cytokines, such as IFN-γ and GM-CSF. They produce various cytokines, such as IL-1, IL-6, TNF-α, IL-10, and IL-12, and other factors, like nitric oxide, ROS, and iNOS, that modulate immune cell activation and differentiation.	50
Mast cells	These cells play a role in allergic reactions and inflammation. They release histamine, tryptase, and other mediators upon activation by IgE bound to allergens. Mast cells also produce cytokines, such as TNF-α, IL-4, IL-5, IL-6, and IL-13, which modulate the function of other immune cells, including T cells and dendritic cells.	51
Monocytes	These circulating cells differentiate into macrophages or dendritic cells upon entering tissues. They participate in phagocytosis and release cytokines, such as IL-1, IL-6, TNF-α, and IL-10, which regulate inflammation and immune responses. Monocytes can be activated by PAMPs, DAMPs, or cytokines, such as GM-CSF and M-CSFs.	52
Neutrophils	These phagocytic cells are the first responders to infection and tissue damage. They release antimicrobial peptides, proteases, and ROS to destroy pathogens. Neutrophils are rapidly recruited to sites of infection or inflammation by chemokines, such as IL-8 and MIP-1 alpha, and other inflammatory mediators produced by epithelial cells, endothelial cells, and other immune cells.	53
Natural Killer (NK) cells	These cytotoxic lymphocytes recognize and kill virus-infected and cancerous cells without prior sensitization. They are activated by cytokines, such as IL-12, IL-15, and IL-18, or by stress-induced ligands on target cells. NK cells produce cytokines, such as IFN-γ, which promote Th1 responses and enhance the cytotoxic activity of CD8+ T cells.	54,55
Adaptive Immunity		
B cells	These cells are responsible for producing and secreting antibodies (IgA, IgE, IgG, etc.) that recognize and neutralize specific pathogens. B cells differentiate into plasma cells upon encountering their specific antigen and receiving help from CD4+ T cells, primarily through CD40L-CD40 interactions and cytokines, such as IL-4, IL-6, and IL-21. Activated B cells can also function as antigen-presenting cells for T cells.	56
Naive CD4+ T cells	Upon activation by dendritic cells presenting antigens via MHC II, naive CD4+ T cells can differentiate into various T helper cell subsets, such as Th1, Th2, Th17, and Tregs. This differentiation is influenced by the cytokine milieu produced by other immune cells, such as dendritic cells, macrophages, and NK cells.	57–59

T helper 1 (Th1) cells	These CD4+ T cells are involved in cell-mediated immunity against intracellular pathogens, such as viruses and some bacteria. They produce IFN-γ and TNF-α, which promote macrophage activation and enhance the cytotoxic activity of CD8+ T cells and NK cells. Th1 cell differentiation is induced by IL-12 and IFN-γ, which are released by antigen-presenting cells, such as dendritic cells and macrophages, in response to intracellular pathogens.	57,58
T helper 2 (Th2) cells	These CD4+ T cells are involved in humoral immunity against extracellular pathogens, such as parasites. They produce IL-4, IL-5, and IL-13, which promote antibody production by B cells, eosinophil activation, and mast cell activation. Th2 cell differentiation is induced by IL-4, which can be released by dendritic cells, basophils, or mast cells.	57,58
T helper 17 (Th17) cells	These CD4+ T cells play a role in defending against extracellular bacterial and fungal infections. They produce cytokines, such as IL-17A, IL-17F, IL-21, and IL-22, which stimulate the production of antimicrobial peptides and the recruitment of neutrophils. Th17 cell differentiation is induced by the cytokines IL-6, TGF-β, IL-1, and IL-23.	57,60
Regulatory T cells (Treg)	These CD4+ T cells play a critical role in maintaining immune tolerance and preventing autoimmunity. They suppress the activation and function of other immune cells, including B cells, CD4+ T cells, CD8+ T cells, and dendritic cells, through various mechanisms, such as the secretion of immunosuppressive cytokines (e.g., TGF-β and IL-10) and direct cell-cell interactions. Treg differentiation is induced by TGF-β and IL-2.	57,58
CD8+ CTL cells	These cytotoxic T cells recognize and kill virus-infected and cancerous cells by releasing cytotoxic granules containing perforin and granzymes. CD8 CTL cell activation requires antigen presentation by MHC I molecules on infected or abnormal cells, as well as help from CD4+ T cells in the form of cytokines, such as IL-2 and IFN-γ.	61,62
NKT cells	These specialized T cells share features of both T cells and NK cells. They recognize lipid antigens presented by the MHC class I-like molecule CD1d and rapidly produce cytokines, such as IFN-γ, IL-4, and IL-17, upon activation. NKT cells play roles in the immune response against various pathogens, tumors, and autoimmune diseases.	63

Immune system stimuli: Common pathogens

Our model also encompasses nine common pathogens from different groups of viruses, bacteria, parasites, and fungi (Table 2). This diversity allows the model to simulate a wide range of infectious diseases and evaluate the immune system's response under different conditions (see Case Study 1). By incorporating pathogen-specific immune responses and host-pathogen interactions at the cellular level, the model provides a realistic representation of the complex interplay between the immune system and invading pathogens.

Table 2: List of pathogen triggers of the modeled immune system.

Cell Type	Brief Synopsis	Citations
Plasmodium falciparum (PF)	The immune response involves innate immunity, with macrophages and neutrophils phagocytosing infected red blood cells. Dendritic cells and NK cells release IFN-γ and TNF-α, promoting parasite killing. Adaptive immunity is mediated by CD4+ T cells producing cytokines like IFN-γ, IL-2, and IL-10, and B cells producing antibodies targeting the parasite.	64,65
Human Papillomavirus (HPV)	The innate immune response includes natural killer cells, macrophages, and dendritic cells. Adaptive immunity involves CD4+ T cells, which produce cytokines like IFN-γ and IL-4, and CD8+ T cells that kill infected cells. B cells produce neutralizing antibodies against the virus.	66
Ebolavirus (EBOV)	Innate immune responses involve macrophages, dendritic cells, and NK cells producing proinflammatory cytokines like TNF-α, IL-6, and IFN-α/β. Adaptive immunity includes CD8+ T cells that target infected cells and CD4+ T cells that produce cytokines like IFN-γ and IL-2, as well as B cells that produce neutralizing antibodies.	67
Mycobacterium tuberculosis (MTB)	The immune response to TB involves macrophages engulfing the bacteria and producing cytokines like TNF-α, IL-1, and IL-6. CD4+ T cells produce IFN-γ and IL-2, activating macrophages to kill intracellular bacteria, while CD8+ T cells target infected cells. B cells produce antibodies, though their role in TB immunity is not fully understood.	68,69
Human Immunodeficiency Virus (HIV)	The immune response to HIV includes innate immunity, with dendritic cells, NK cells, and macrophages producing IFN-α/β and other cytokines. Adaptive immunity involves CD8+ T cells that target infected cells and CD4+ T cells that produce cytokines like IFN-γ and IL-2. B cells produce neutralizing antibodies, but HIV's high mutation rate allows it to evade the immune system.	70
Ascaris lumbricoides (AL)	These parasitic worms trigger a Th2 immune response, with CD4+ T cells producing cytokines like IL-4, IL-5, and IL-13. This response activates eosinophils, mast cells, and basophils, which release inflammatory mediators and granules to damage the worms. B cells produce IgE antibodies that bind to the parasites, facilitating their destruction by eosinophils and other immune cells.	71
Leishmania donovani (LD)	The immune response involves macrophages, which phagocytose the parasites and produce cytokines like TNF-α and IL-1. CD4+ T cells are crucial for immunity against Leishmania, with Th1 cells producing IFN-γ and IL-2, activating macrophages to kill intracellular parasites, while Th2 cells can promote disease progression. CD8+ T cells and B cells also play roles in the immune response, with CD8+ T cells targeting infected cells and B cells producing antibodies.	72
Influenza A Virus (IAV)	The immune response begins with the innate system, including macrophages, dendritic cells, and NK cells, which produce cytokines like IFN-α/β, TNF-α, and IL-6. Adaptive immunity involves CD4+ T cells producing cytokines like IFN-γ and IL-2, CD8+ T cells targeting infected cells, and B cells producing neutralizing antibodies against viral surface proteins, such as hemagglutinin and neuraminidase.	73

Candida albicans (CA)	The immune response involves the activation of innate immune cells like neutrophils, macrophages, and dendritic cells that produce cytokines like TNF-α, IL-1, and IL-6. Adaptive immunity is mediated by CD4+ T cells, with Th1 cells producing IFN-γ and Th17 cells producing IL-17 and IL-22, which stimulate the production of antimicrobial peptides and recruit neutrophils. B cells produce antibodies, though their role in anti-Candida immunity is less clear.	74

These pathogens trigger various immune responses involving both innate and adaptive immune cells, as well as the release of cytokines, chemokines, and other molecules that help coordinate the immune response. Understanding the immune response to these pathogens is crucial for developing effective treatments and vaccines to combat infectious diseases.

Systems Biology Graphical Notation Map

We created a Systems Biology Graphical Notation (SBGN) map of the model, visually representing the immune system components and their interactions. This SBGN map facilitates the understanding of the model structure and supports its use by researchers with varying levels of expertise in computational biology. Figure 2 presents a detailed visualization of the intricate web of signals and responses that govern the immune system's defense against infections. As depicted in Figure 2a, the map is structured into five discrete tiers, namely pathogens, non-immune target cells, innate immune cells, adaptive immune cells, and secreted molecules, to facilitate the interpretation of the information. Figure 2b provides a network view of the map, illustrating the comprehensive set of 197 components and 614 reactions that interplay among these components. Additionally, Figure 2c presents a zoom-in view of the map that shows secreted cytokines and immunoglobulins. A range of cytokines and immunoglobulins, including CXCL10, IL1B, IFNB1, PAF1, IFNA1, IL15, IL12A, IL18, IL10, IL2, IFNG, IL25, CCL3, IL13, IL33, IL5, IL4, IgA, IgE, IGg, TGFB1, TNF, IL27, IL1A, CXCL8, IL6, IL21, IL23A, IL22, IL17F, IL17A, CSF1, CSF2, and CSF3, are involved in cell-cell communication within this network. This detailed depiction provides a comprehensive framework for understanding the immune response and has implications for the development of novel therapeutic interventions.

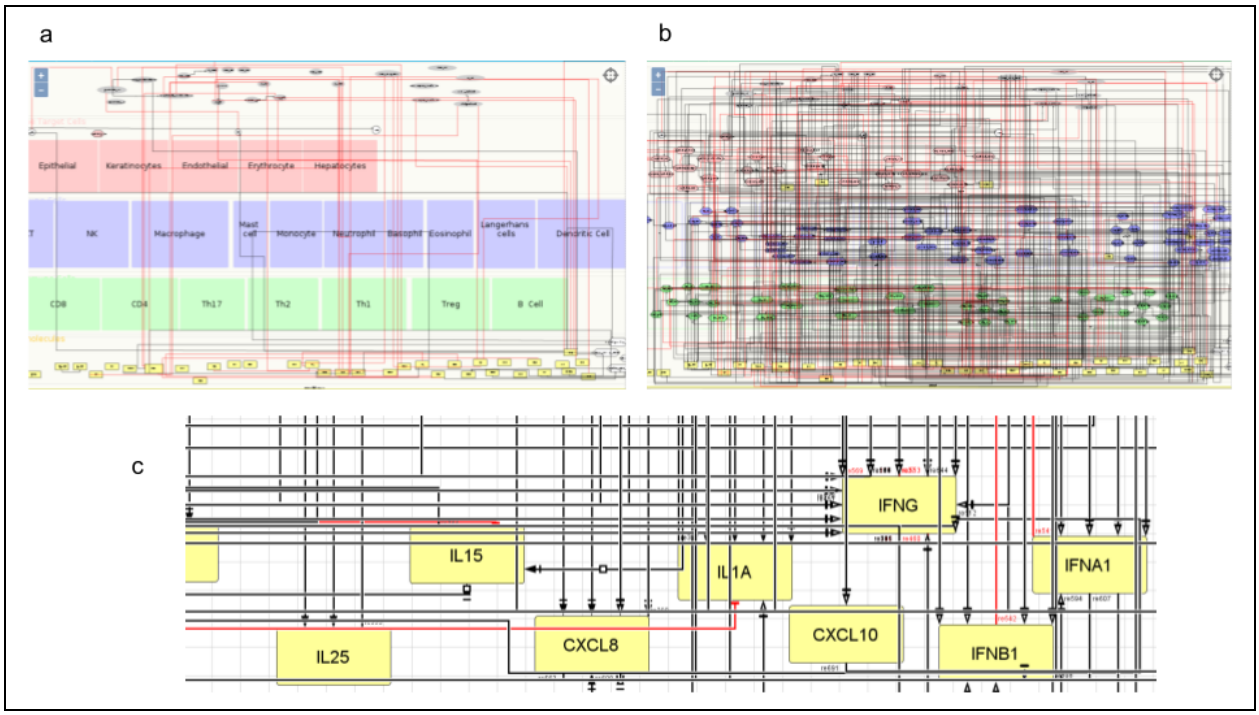

Figure 2-a) Zoom-out view of the IDT map with cell type layers b) Network view of the map. The gray, pink, purple, green, and yellow nodes in the network present pathogens, non-immune target cells, innate immune cells, adaptive immune cells, and secreted molecules, respectively. The red interactions show the inhibitions, and the black ones are the activations. c) Zoom-in view of the secreted proteins.

Model Availability

The model is available on the Cell Collective platform, a user-friendly online environment for building, simulating, and analyzing computational models of biological systems, allowing researchers to access, modify, and utilize the model for their specific research questions (https://cellcollective.org/#module/91515:1/immune-system-model/1).

B. Model validation

To evaluate the accuracy and reliability of the computational model, we compared its predictions with real-world experimental data. These included data from *in vitro* and *in vivo* studies, as well as clinical observations, encompassing various aspects of immune responses to the selected pathogens. By comparing the model's output with experimental results, we assessed its ability to accurately simulate the dynamics of innate and adaptive immune cells, cytokines, immunoglobulins, and host-pathogen interactions during infections.

First, we assessed and confirmed the model's ability to simulate the proper immune response to each pathogen as characterized in the literature. Table 1 shows the cell target, predicted immune responses, and the literature support to confirm the prediction for each of the nine pathogens. For example, all pathogens showed both Th1-specific immune responses, whereas helminths showed Th1 and Th2-specific immune responses. During helminth infection,

antigen-presenting cells (APCs), such as macrophages, capture and process the antigens, presenting them to the CD4+ T cells. The CD4+ T cells differentiate into Th2 cells and produce cytokines such as IL-4, IL-5, and IL-13. These cytokines activate B cells to produce IgE antibodies, which bind to the helminth antigens.[75] Our model showed the activity of Macrophages and Th2 cells in response to helminth infection and produced IgE antibodies (Table 3). Similarly, the target cells aligned well with the literature for all other pathogens.

Table 3: Cell target and immune response to each of the pathogens.

Infectious Agent	Cell Target or Innate immune response	Adaptive Immune Response	Reference
HIV	Dendritic Cells, Macrophages	Th1, CD8+	[76]
Human papillomavirus	Keratinocytes	Th1, CD8+	[77]
Ebola	Dendritic Cells, Macrophages, Monocytes	Th1, CD8+, IgG	[78]
Influenza A virus	Epithelial, Dendritic	Th1, CD8+, IgA, IgG, IgM	[79]
Mycobacterium tuberculosis	Macrophages, Neutrophil cells	Th1, CD8+	[80]
Helminth	Endothelial, Epithelial, Macrophages, NKT	Th2, IgE, IgG	[81]
Plasmodium falciparum	Erythrocytes	Th1, IgE, IgG	[82,82,83]
Leishmania	Dendritic Cells, Macrophages, Monocytes, Neutrophil, NK	Th1, IgE	[72]
Candida albicans	Macrophages	Th17	[84]

Next, we simulated cytokine and immunoglobulin production in response to each infection (Figure 2A) and compared it with the literature. EBOV infection stimulates a stronger response of both pro-inflammatory cytokines (IL-1, IL-6, and IL-12) and anti-inflammatory cytokines (IL-8 and IL-10). This response aligned with experimental data [78,85]. HPV infection stimulates a strong response of anti-inflammatory cytokines IL-10 and TGF-β. The higher activity of IL-10 during HPV infection is congruent with studies suggesting a role for IL-10 in immune evasion through an immunosuppressive state [86]. AL infection results in a strong anti-inflammatory response (IL-10, IL-4, IL-13, and IL-5) which aligns with the literature. However, the production of IL-4 and IL-5 was higher in the patient group [87]. IAV infection stimulates a robust pro-inflammatory response (IL-1, IL-6, IL-12, IL-18, and TNF-α). IAV infects alveolar macrophages in the lower respiratory tract, which secretes many of these pro-inflammatory cytokines [88]. Cytokine response to PF is mixed pro- and anti-inflammatory, which aligns with the literature since both pro and anti-inflammatory responses are important in the immune response against malaria [89]. MTB induces a strong pro-inflammatory cytokine response that also aligns with the literature [90]. In our model, the cytokine and immunoglobulin response to HIV is not significant because of the infection-driven, low activation of immune cells (e.g., CD4+ T cells) mimicking the stage of disease with immunodeficiency. Among all cytokines, IL-10, IFN-γ, and TNF-α were identified

as the most active in response to simulated infection by different pathogens, being active in response to eight, seven, and five modeled pathogens, respectively (Figure 2A).

IL-10 (Figure 2B): We observed increased IL-10 activity in response to simulated infection by HPV, EBOV, AL, PF, IAV, and MTB. Medium to high doses of HPV triggered the highest response of IL-10. Increased doses of EBOV corresponded to a linear increase of IL-10. We observed similar linear increases in response to AL and PF, but the IL-10 activity levels were lower than with EBOV. The activity of IL-10 decreased with increased doses of LD.

IFN-γ: IFN-γ activity increased proportionally to the doses of MTB, PF, and LD. (Figure 2C). MTB triggered the highest IFN-γ response. Low to medium dosage of EBOV triggered high activities of IFN-γ, which subsequently decreased at a high dose. We observed a slight increase in IFN-γ response in response to HPV and HIV and low IFN-γ activity in response to high doses of CA.

TNF-α (Figure 2D): TNF-α activity increased proportionally to the doses of EBOV, PF, IAV, and MTB. In contrast, TNF-α activity initially increased and then decreased with increased doses of LD. We observed the highest TNF-α activity in response to EBOV infection.

These patterns aligned well with the literature. For example, in HPV infection, we observed an increase in IL-10 activity (Figure 2B) and a decrease in IFN-γ activity (Figure 2C). This observation is supported by literature as HPV infects primitive basal keratinocytes [66] that produce IL-10, further facilitating the infection process via a positive feedback loop between IL-10 and HPV transcription [86]. At the same time, HPV downregulates the expression of IFNs [91].

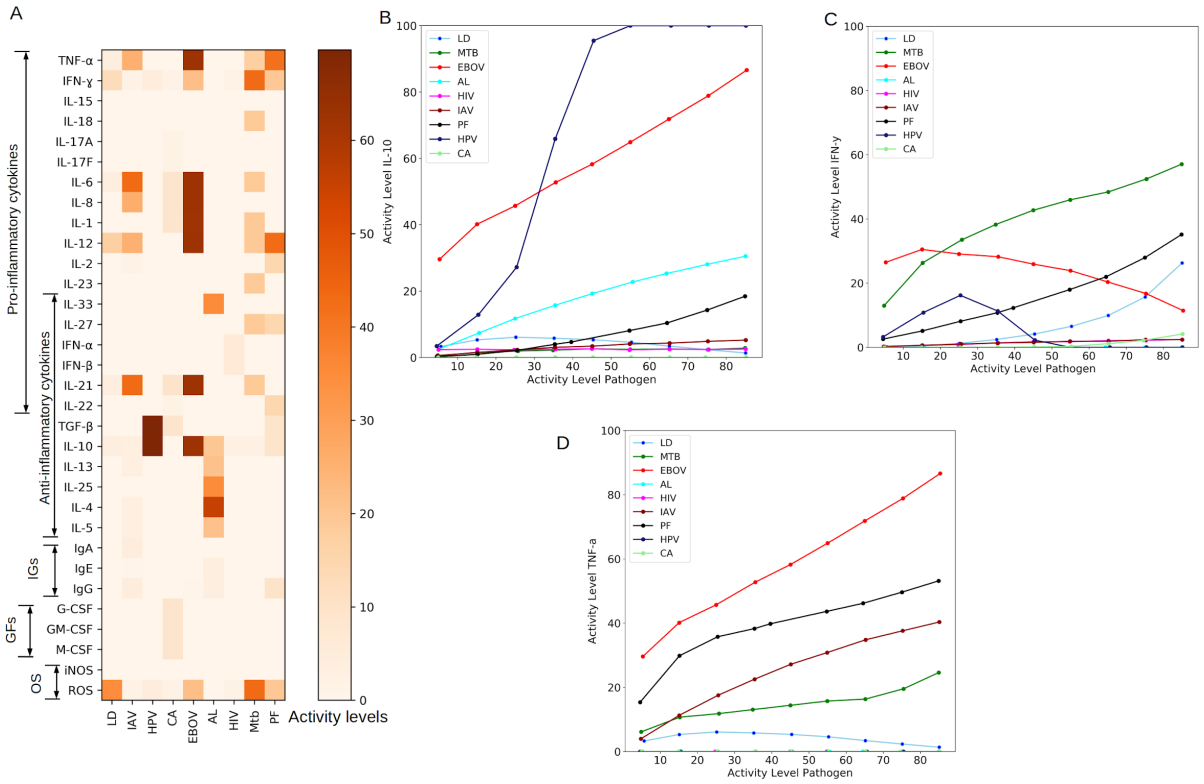

Figure 2: Immune response to single pathogen infections. (A) Activity levels of cytokines upon infection. Activity levels vary from 0% (no activity) to 100% (highest activity). The activity levels represent the average value triggered by pathogen levels from 0 - 100%. IGs = immunoglobulins, GFs = growth factors, OS = oxidative stress. (B, C, and D) Dynamics of cytokines IL-10, IFN-γ, and TNF-α in response to different activity levels of pathogens.

Furthermore, we assessed the model's ability to reproduce more specific experimental observations from the literature. For example, we present validation results for the case of *M. tuberculosis* infection. IFN-γ has been demonstrated as essential for resistance against MTB infection [92]. Consistent with this finding, our model's simulation results indicate that knocking out IFN-γ indeed leads to increased replication of M. tuberculosis (Figure 3A). Additionally, we reproduced 11 complex scenarios from experimental literature (Supplementary Table 1).

In summary, the model accurately replicated the immune responses for nine different pathogens, including HIV, Ebola, Influenza A virus, and Mycobacterium tuberculosis, among others. It also correctly simulated cytokine and immunoglobulin production in response to each infection, aligning with the literature. Notably, it demonstrated its ability to reproduce complex experimental scenarios, such as the increased replication of M. tuberculosis in the absence of IFN-γ. Overall, the model showed a high level of accuracy and reliability in simulating immune responses to infections.

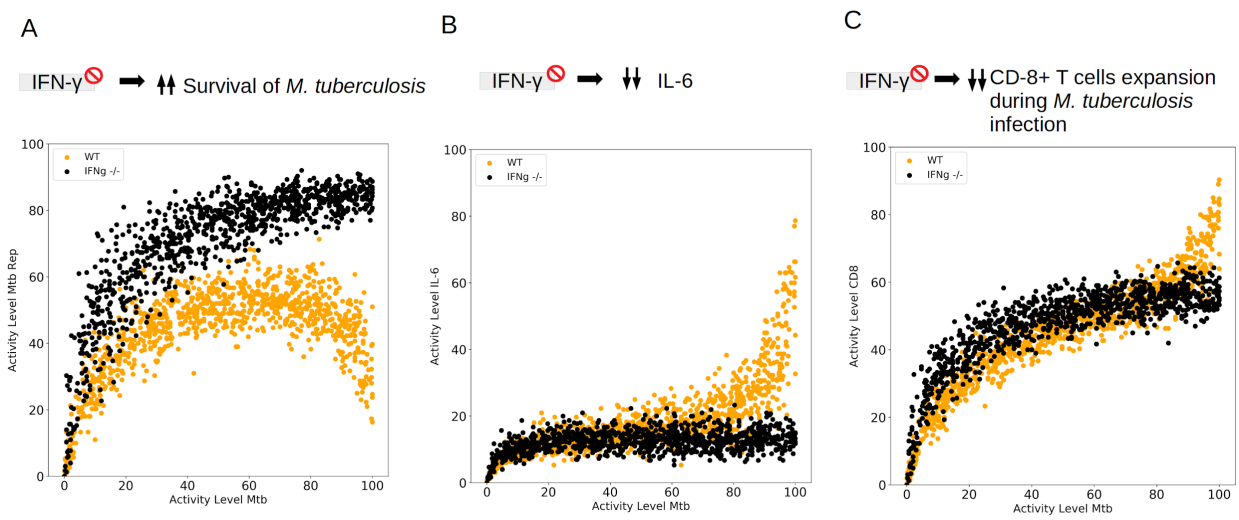

Figure 3: Model validation. Each panel presents literature observations following IFN-γ knock-outs, along with corresponding model simulation results compared to wild type (WT). (A) Activity levels of M. tuberculosis replication (Y-axis) in the presence (WT) and absence (IFN-γ -/-) of IFN-γ. (B) IL-6 activity levels (Y-axis) under both WT and IFN-γ knock-out conditions. (C) CD8 cell activity in the context of WT and IFN-γ knock-out conditions.

C. Case Study: Immune response to various coinfections

Understanding the immune response to coinfections is crucial for several reasons. Coinfections can complicate clinical presentation, diagnosis, and treatment, often resulting in more severe symptoms and increased morbidity or mortality. Characterizing immune responses to coinfections allows researchers to identify key differences in cytokine and immunoglobulin activity levels depending on the infection order. These insights can lead to more effective therapies and targeted interventions, improving patient outcomes. Furthermore, examining the immune system's behavior during coinfections provides valuable information on the complex interplay between various pathogens and the host's immune system. This knowledge can help researchers better understand the mechanisms behind immune system regulation, identify potential vulnerabilities, and design innovative strategies to prevent or manage coinfections. In an era of emerging and re-emerging infectious diseases, understanding the immune response to coinfections is paramount to global public health.

Response of specific cytokines to coinfections depends on the order of infections

We analyzed the model's dynamics in response to 17 medically relevant (observed) sequential coinfections (refer to Supplementary Table 2 and Materials and Methods). For each coinfection, we reversed the infection order and compared cytokine and immunoglobulin activity levels. We found that cytokine and immunoglobulin activity levels significantly differ when the infection order is reversed (Figures 4A and 4B). We conducted two types of analysis:

First, we explored which coinfection pairs exhibited the highest number of differentially active immune molecules upon reversing the infection order. We discovered that IAV-PF and HIV-CA coinfections were most order-sensitive, resulting in 21 (out of 32) modeled cytokines and immunoglobulins exhibiting significantly different activity levels. AL-MTB, CA-MTB, and IAV-MTB coinfections led to 20 differentially active cytokines and immunoglobulins. Infection order was least important for MTB-LD and HIV-LD coinfections, where only 10 and 11 cytokines and immunoglobulins, respectively, displayed differential activities. The top two coinfections shared 13 differentially activated cytokines and immunoglobulins, while the bottom two shared seven. The number of infection order-sensitive cytokines in all studied coinfection pairs is shown in Figure 5A.

Second, we examined specific cytokines and immunoglobulins most impacted by infection order. IL-10 was strongly affected by the order in all infection pairs. IFN-γ, IL-12, ROS, TNF-α, IL-18, IL-21, IL-6, IFN-α, IFN-β, IL-27, IL-23, IL-1, and TGF-β were also significantly affected. The order of coinfections significantly influenced IFN-γ, IL-12, and ROS activities in 16 out of 17 pairs, TNF-α and IL-18 activities in 15 pairs, and IL-21 activity in 14 pairs. Only iNOS activity was not significantly impacted by any coinfections order (Figure 5B).

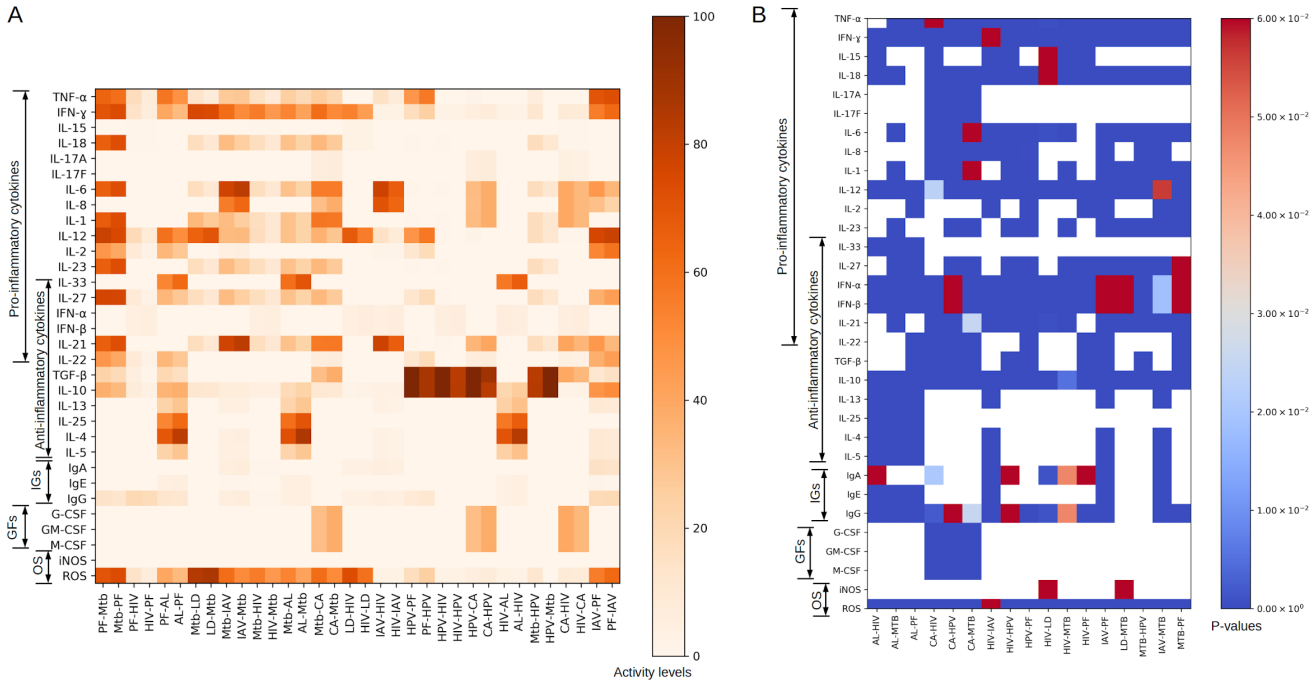

Figure 4: Immune response to coinfections. (A) Activity levels of cytokines in response to coinfection pairs. (B) P-values of compared activity profiles under a different order of infecting pathogens. White cells represent the components inactive during coinfection. IGs = immunoglobulins, GFs = growth factors, OS = oxidative stress.

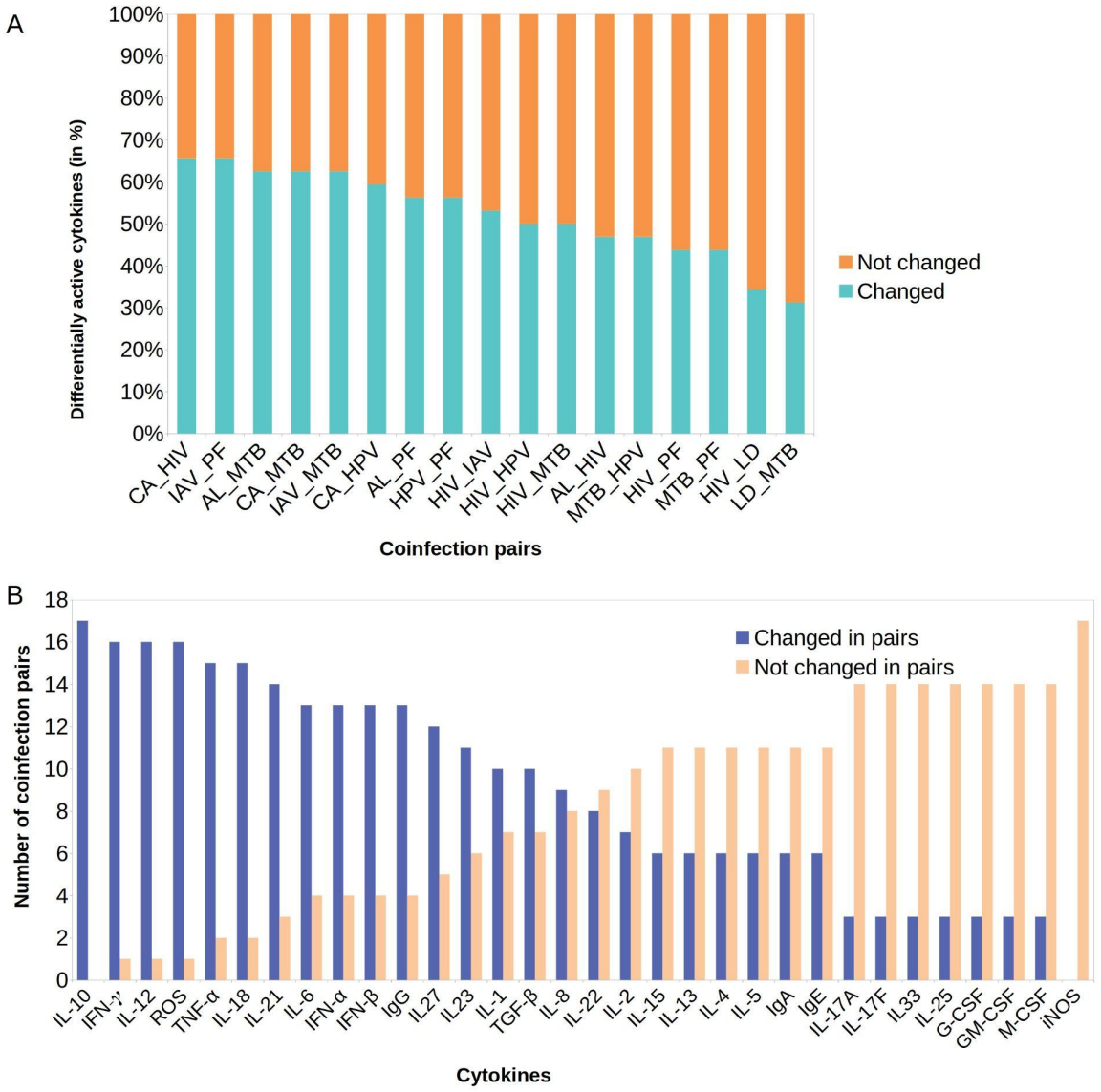

Figure 5: Differentially active cytokines under different coinfections: (A) % of differentially active cytokines (out of 32) under different coinfections. Turquoise = % of 32 cytokines showing differential activity levels. Orange = % of 32 cytokines not showing differential activity levels. (B) # coinfection pairs' orders showing differential activity for each cytokine (out of 17 pairs). Blue = coinfection pairs' orders affecting cytokine activities. Brown= coinfection pairs' orders not affecting cytokine activities.

One pathogen is dominant in most coinfection pairs

Next, we used hierarchical clustering and principal component analysis (PCA) to determine the dominant pathogens and cytokines in coinfections. We utilized cytokine and immunoglobulin activity levels obtained under high infection strength (90-100%) across different orders of coinfections. The clustering analysis yielded five clusters, reversed orders of the same coinfection clustering together (Figure 6A). Cluster 1 is dominated by HPV coinfections, Cluster

2 by AL, and Cluster 3 by both MTB and LD. Cluster 4 consists of two PF coinfections, while Cluster 5 contains four coinfections (two with MTB and two with HIV). PC1 and PC2 accounted for 57% of the data variance (Figures 6C and 6D). Both PC1 and PC2 exhibited high scores for coinfections in Cluster 1 (dominated by HPV). PC1 was associated with strong loadings of anti-inflammatory cytokines (TGF-β and IL-10) versus pro-inflammatory loadings (IL-6, IL-12, IL-18, IFN-γ), while PC2 aligned with different groups of anti-inflammatory cytokines, such as TGF-β and IL-10 versus IL-4 and IL-25.

These findings demonstrate that HPV and AL dominated the immune response over other infections regardless of their order in the coinfection. Coinfection clustering was influenced by cytokines exhibiting variability in more than 50% of coinfections (as discussed in the previous section and illustrated in Figure 5), including IL-10, TGF-β, ROS, IFN-γ, IL-12, and TNF-α.

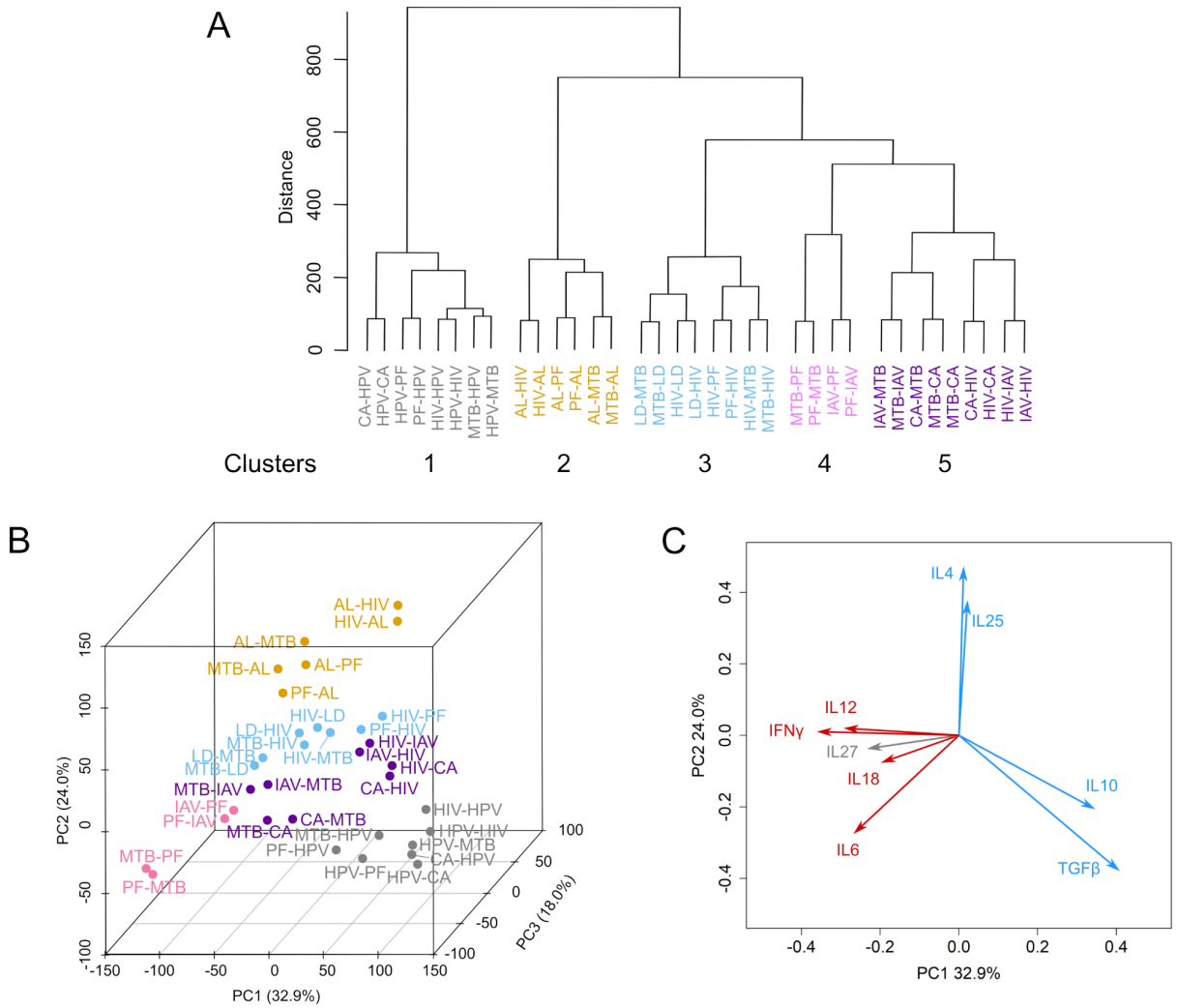

Figure 6: Clustering of coinfections (A) Hierarchical clustering of coinfections, distance = dissimilarity between coinfections. (B) Principal component analysis. (D) Main cytokine loadings upon PC1 and PC2. Red = pro-inflammatory, blue = anti-inflammatory.

By identifying the dominant pathogens in coinfections (e.g., Human papillomavirus and Ascaris lumbricoides) and the key cytokines influencing coinfection clustering, researchers can better understand the complex interactions between pathogens and the immune response during coinfections. For example, the study provides insights into how different pathogens interact with one another during coinfections, which can be vital for understanding the mechanisms behind disease progression and severity. This information can help scientists identify potential synergistic or antagonistic effects between pathogens that may influence the overall course of the disease. Further, identifying the cytokines that play a critical role in coinfections can contribute to the development of immunomodulatory therapies. By targeting these specific cytokines, it may be possible to enhance the immune system's ability to combat coinfections, reduce inflammation, or prevent adverse immune reactions. Finally, recognizing the dominant pathogens and cytokines involved in coinfections can aid in the development of more accurate diagnostic tools and targeted therapies. By focusing on these key factors, clinicians can tailor treatments to address the specific immune response triggered during coinfections, potentially improving patient outcomes.

Discussion

The immune system is a highly complex and dynamic network, spanning multiple temporal scales and levels of biological organization. Developing an accurate and comprehensive digital twin of the immune system necessitates a solid foundation that incorporates the essential cellular components and their interactions. The logical model and blueprint presented in this study serve as this foundation, ensuring that the innate and adaptive immune cells, cytokines, immunoglobulins, and other components of the immune system are accurately represented before introducing additional levels of complexity. As the community continues its efforts towards implementing immune digital twins and including other levels of biological organization, the blueprint will serve as a guide for constructing the multi-scale model. The immune system is an area of active research stemming from many different disciplines, including immunology and computational biology. A comprehensive blueprint of the immune system can facilitate collaboration among these researchers by providing a common framework and language for understanding the system's complexity and interactions.

We validate the cellular-level logical model against available experimental data to assess their accuracy in representing the immune system's response to different modeled pathogens, which include bacteria, viruses, and parasites. This assessment allowed us to gauge how well the model captures the complexities and interactions within the immune system when faced with different types of infections. For instance, the model was able to reproduce the activation and differentiation of T cells in response to viral infections, as well as the recruitment and activation of neutrophils during bacterial infections.

Despite the compelling advantages of logical modeling, there are some limitations to the modeling approach. For example, logical models are qualitative in nature and therefore lack the quantitative precision required to model the kinetics of immune responses. Furthermore, the construction of logical models is heavily dependent on the current state of knowledge and may therefore lack components or interactions that have not yet been discovered or fully understood. On the other hand, logical models provide numerous benefits, particularly in their ability to

capture complex systems in a simplified and computationally efficient manner. They are especially useful for systems with incomplete kinetic data, as they allow for studying system-level behavior based on the known structure of the regulatory network. Logical models can be used to generate hypotheses about the system's behavior, which can then be tested experimentally. Moreover, they are valuable tools for identifying key regulatory components and potential intervention points in the system.

While the immune digital blueprint model provides a comprehensive representation of many key immune system components and their interactions, it is important to acknowledge that it is not an exhaustive depiction of the entire immune system. There are still many cellular and molecular components, as well as interactions that have not been included in the current model. The immune system model is also limited to pathogens as triggers for an immune response. For example, other specialized subsets of T cells, such as follicular helper T cells (Tfh) and resident memory T cells (Trm), are not explicitly represented in the current model. Similarly, the model doesn't explicitly represent how immune cells move through different compartments or how the local tissue environment influences cell behavior. However, the model is primarily designed to capture the core, broadly applicable aspects of the immune system functioning against a variety of insults. Our validation exercises have shown that these key immune responses can be accurately represented even without these additional cell types and states. Thus, while these components could provide additional granularity and potentially enable the model to address more specific questions in future iterations, their absence does not undermine the model's current accuracy or utility in simulating the general patterns of the immune response. Furthermore, the model’s accessibility in Cell Collective and through SBML provides an opportunity for the community to continue to refine and expand the model to enable simulations of the immune response to other insults, such as allergies, autoimmune conditions, and trauma.

The current blueprint model focuses primarily on the cellular level of the immune system. To provide a more comprehensive understanding of the immune system, future work should aim to integrate multi-scale modeling approaches, encompassing molecular, cellular, tissue, organ, and organism levels. By incorporating information from these various scales, researchers can develop a more holistic understanding of the immune system and its role in health and disease. Including physiologically based pharmacokinetics/pharmacodynamics (PBPK/PD), for instance, would allow the model to predict the effects of drug interventions on the immune system and how these effects might vary among different individuals or under different physiological conditions.

For example, we recently created the first draft of a multicellular, multi-scale, and multi-approach computational model of CD4+ T-cells [93], which can serve as a computational framework for implementing additional scales atop the cellular-level blueprint model presented here. This multi-scale framework integrates physiological (ordinary differential equations), cellular (agent-based approaches), molecular (stochastic logical approach), and genome-level (constraint-based approach) models with heterogeneous high-throughput datasets and bioinformatics algorithms. The model also represents various compartments, such as the site of initial insult/infection (e.g., lungs for infectious diseases), lymphoid tissues connected to the site of insult (a micro-environment where antigens can stimulate antigens), and the circulatory

system. The multi-scale and multicellular model demonstrated mathematically and computationally how information flows within and across scales in a single integrated framework, validated by reproducing observed responses of naive CD4+ T cells to different combinations of cytokines. [93]

The cellular-level blueprint immune system model will guide the expansion of the aforementioned multi-scale, multicellular framework by expanding it by incorporating additional immune cell-specific sub-models of genome-scale metabolism and signal transduction. While a few such models already exist (e.g., signal transduction network models of antigen-presenting cells[40], CD4+ effector T cells [57], and Macrophages [94] and constraint-based metabolic models of Th1, Th2, Th17, and regulatory T cells[95,96] and macrophages[97]), the majority of sub-models of other immune cells will need to be developed.

Future multi-scale general-purpose immune digital twin to be applied to many immune-related conditions, including autoimmune diseases and primary immune disorders, infectious diseases, cancer immunotherapy, chronic diseases, wound healing, transplantation, and trauma responses. By considering the immune digital twin scope within these areas, researchers can explore the immune system's involvement in these processes and identify potential interventions to improve patient outcomes. For example, the model could be used to simulate the immune response during wound healing to optimize wound care strategies, or to predict the risk of graft rejection in transplantation settings, leading to better patient management and improved clinical outcomes.

Conclusion

This study provides a comprehensive map and a simulatable logical model of the immune system, serving as the first blueprint for an immune system digital twin. This blueprint integrates 27 innate and adaptive immune cells, 31 cytokines and immunoglobulins, and 9 different pathogens, providing a solid foundation for developing a multi-scale model. We demonstrated the model's potential in characterizing system-wide immune responses to various coinfections. By making the model available in easy-to-use formats directly in Cell Collective and as an SBGN map, it can be easily further expanded by the community.

The presented cellular-level blueprint of the immune system represents a significant step toward the development of general-purpose immune digital twins. The development and application of immune digital twins have far-reaching implications for the future of digital twin technology in life sciences and healthcare. As digital twins continue to advance, they have the potential to advance patient care and accelerate the transition toward precision medicine. By integrating diverse data sources and providing comprehensive, dynamic models, digital twins enable researchers and healthcare professionals to investigate system behavior, optimize treatments, and develop innovative solutions to pressing medical challenges. Furthermore, digital twins can facilitate collaboration among researchers from different disciplines, providing a common framework and language to understand the complexities and interactions of biological systems.

References Cited

1. Wu, C. *et al.* MRI-Based Digital Models Forecast Patient-Specific Treatment Responses to Neoadjuvant Chemotherapy in Triple-Negative Breast Cancer. *Cancer Res.* **82**, 3394–3404 (2022).

1. Ferdousi, R., Laamarti, F. & El Saddik, A. Chapter 6 - Artificial intelligence models in digital twins for health and well-being. in *Digital Twin for Healthcare* (ed. El Saddik, A.) 121–136 (Academic Press, 2023). doi:10.1016/B978-0-32-399163-6.00011-1.
2. Sun, T., He, X. & Li, Z. Digital twin in healthcare: Recent updates and challenges. *Digit. Health* **9**, 20552076221149652 (2023).
3. Singh, M. *et al.* Applications of Digital Twin across Industries: A Review. *Appl. Sci.* **12**, 5727 (2022).
4. Raj, P. & Surianarayanan, C. Chapter Twelve - Digital twin: The industry use cases. in *Advances in Computers* (eds. Raj, P. & Evangeline, P.) vol. 117 285–320 (Elsevier, 2020).
5. Guo, J. & Lv, Z. Application of Digital Twins in multiple fields. *Multimed. Tools Appl.* **81**, 26941–26967 (2022).
6. Haleem, A., Javaid, M., Pratap Singh, R. & Suman, R. Exploring the revolution in healthcare systems through the applications of digital twin technology. *Biomed. Technol.* **4**, 28–38 (2023).
7. Sahal, R., Alsamhi, S. H. & Brown, K. N. Personal Digital Twin: A Close Look into the Present and a Step towards the Future of Personalised Healthcare Industry. *Sensors* **22**, 5918 (2022).
8. Papachristou, N. *et al.* Digital Transformation of Cancer Care in the Era of Big Data, Artificial Intelligence and Data-Driven Interventions: Navigating the Field. *Semin. Oncol. Nurs.* 151433 (2023) doi:10.1016/j.soncn.2023.151433.

9. Stahlberg, E. A. *et al.* Exploring approaches for predictive cancer patient digital twins: Opportunities for collaboration and innovation. *Front. Digit. Health* **4**, 1007784 (2022).
10. Wang, J., Qiao, L., Lv, H. & Lv, Z. Deep Transfer Learning-based Multi-modal Digital Twins for Enhancement and Diagnostic Analysis of Brain MRI Image. *IEEE/ACM Trans. Comput. Biol. Bioinform.* **PP**, (2022).
11. Wu, C. *et al.* MRI-Based Digital Models Forecast Patient-Specific Treatment Responses to Neoadjuvant Chemotherapy in Triple-Negative Breast Cancer. *Cancer Res.* **82**, 3394–3404 (2022).
12. Hormuth, D. A. *et al.* Math, magnets, and medicine: enabling personalized oncology. *Expert Rev. Precis. Med. Drug Dev.* **6**, 79–81 (2021).
13. Hernandez-Boussard, T. *et al.* Digital Twins for Predictive Oncology will be a Paradigm Shift for Precision Cancer Care. *Nat. Med.* **27**, 2065–2066 (2021).
14. Zahid, M. U. *et al.* Forecasting Individual Patient Response to Radiation Therapy in Head and Neck Cancer With a Dynamic Carrying Capacity Model. *Int. J. Radiat. Oncol. Biol. Phys.* **111**, 693–704 (2021).
15. Levine, S. *et al.* Dassault Systèmes' Living Heart Project. in *Modelling Congenital Heart Disease: Engineering a Patient-specific Therapy* (eds. Butera, G., Schievano, S., Biglino, G. & McElhinney, D. B.) 245–259 (Springer International Publishing, 2022). doi:10.1007/978-3-030-88892-3_25.
16. Arduini, M. *et al.* Framework for patient-specific simulation of hemodynamics in heart failure with counterpulsation support. *Front. Cardiovasc. Med.* **9**, 895291 (2022).
17. Coorey, G., Figtree, G. A., Fletcher, D. F. & Redfern, J. The health digital twin: advancing precision cardiovascular medicine. *Nat. Rev. Cardiol.* **18**, 803–804 (2021).
18. Shamanna, P. *et al.* Type 2 diabetes reversal with digital twin technology-enabled precision nutrition and staging of reversal: a retrospective cohort study. *Clin. Diabetes Endocrinol.* **7**, 21 (2021).

19. Silfvergren, O. *et al.* Digital twin predicting diet response before and after long-term fasting. *PLOS Comput. Biol.* **18**, e1010469 (2022).
20. Brown, S. A. *et al.* Six-Month Randomized, Multicenter Trial of Closed-Loop Control in Type 1 Diabetes. *N. Engl. J. Med.* **381**, 1707–1717 (2019).
21. Kovatchev, B. A Century of Diabetes Technology: Signals, Models, and Artificial Pancreas Control. *Trends Endocrinol. Metab. TEM* **30**, 432–444 (2019).
22. Laubenbacher, R. *et al.* Building digital twins of the human immune system: toward a roadmap. *Npj Digit. Med.* **5**, 1–5 (2022).
23. Novère, N. L. *et al.* The Systems Biology Graphical Notation. *Nat. Biotechnol.* **27**, 735–741 (2009).
24. Matsuoka, Y., Funahashi, A., Ghosh, S. & Kitano, H. Modeling and simulation using CellDesigner. *Methods Mol. Biol. Clifton NJ* **1164**, 121–145 (2014).
25. Seal, R. L. *et al.* Genenames.org: the HGNC resources in 2023. *Nucleic Acids Res.* **51**, D1003–D1009 (2023).
26. Keating, S. M. *et al.* SBML Level 3: an extensible format for the exchange and reuse of biological models. *Mol. Syst. Biol.* **16**, e9110 (2020).
27. Gawron, P. *et al.* MINERVA-a platform for visualization and curation of molecular interaction networks. *NPJ Syst. Biol. Appl.* **2**, 16020 (2016).
28. Morris, M. K., Saez-Rodriguez, J., Sorger, P. K. & Lauffenburger, D. A. Logic-Based Models for the Analysis of Cell Signaling Networks. *Biochemistry* **49**, 3216–3224 (2010).
29. Abou-Jaoudé, W. *et al.* Logical Modeling and Dynamical Analysis of Cellular Networks. *Front. Genet.* **7**, 94 (2016).
30. Helikar, T., Konvalina, J., Heidel, J. & Rogers, J. A. Emergent decision-making in biological signal transduction networks. *Proc. Natl. Acad. Sci. U. S. A.* **105**, 1913–1918 (2008).
31. Helikar, T., Kochi, N., konvalina, john & A. Rogers, J. Boolean Modeling of Biochemical Networks. *Open Bioinforma. J.* **5**, 16–25 (2011).

32. Helikar, T. *et al.* The Cell Collective: Toward an open and collaborative approach to systems biology. *BMC Syst. Biol.* **6**, 96 (2012).
33. Chaouiya, C. *et al.* SBML qualitative models: a model representation format and infrastructure to foster interactions between qualitative modelling formalisms and tools. *BMC Syst. Biol.* **7**, 135 (2013).
34. Chaouiya, C. *et al.* SBML Level 3 package: Qualitative Models, Version 1, Release 1. *J. Integr. Bioinforma.* **12**, (2015).
35. Helikar, T. & Rogers, J. A. ChemChains: a platform for simulation and analysis of biochemical networks aimed to laboratory scientists. *BMC Syst. Biol.* **3**, 58 (2009).
36. Todd, R. G. & Helikar, T. Ergodic Sets as Cell Phenotype of Budding Yeast Cell Cycle. *PLOS ONE* **7**, e45780 (2012).
37. Galli, S. J. & Tsai, M. IgE and mast cells in allergic disease. *Nat. Med.* **18**, 693–704 (2012).
38. Siracusa, M. C., Kim, B. S., Spergel, J. M. & Artis, D. Basophils and allergic inflammation. *J. Allergy Clin. Immunol.* **132**, 789–801; quiz 788 (2013).
39. Liu, K. Dendritic Cells. *Encycl. Cell Biol.* 741–749 (2016) doi:10.1016/B978-0-12-394447-4.30111-0.
40. Aghamiri, S. S., Puniya, B. L., Amin, R. & Helikar, T. A multiscale mechanistic model of human dendritic cells for in-silico investigation of immune responses and novel therapeutics discovery. *Front. Immunol.* **14**, 1112985 (2023).
41. Mai, J., Virtue, A., Shen, J., Wang, H. & Yang, X.-F. An evolving new paradigm: endothelial cells--conditional innate immune cells. *J. Hematol. Oncol.J Hematol Oncol* **6**, 61 (2013).
42. Bhavsar, I., Miller, C. S. & Al-Sabbagh, M. Macrophage Inflammatory Protein-1 Alpha (MIP-1 alpha)/CCL3: As a Biomarker. *Gen. Methods Biomark. Res. Their Appl.* 223–249 (2015) doi:10.1007/978-94-007-7696-8_27.
43. Kita, H. EOSINOPHILS: MULTIFACETED BIOLOGIC PROPERTIES AND ROLES IN HEALTH AND DISEASE. *Immunol. Rev.* **242**, 161–177 (2011).

44. Heijink, I. H. *et al.* Epithelial cell dysfunction, a major driver of asthma development. *Allergy* **75**, 1902–1917 (2020).

45. Zhou, Z., Xu, M.-J. & Gao, B. Hepatocytes: a key cell type for innate immunity. *Cell. Mol. Immunol.* **13**, 301–315 (2016).

46. Jin, J., Sunusi, S. & Lu, H. Group 2 innate lymphoid cells (ILC2s) are important in typical type 2 immune-mediated diseases and an essential therapeutic target. *J. Int. Med. Res.* **50**, 03000605211053156 (2022).

47. Jiang, Y. *et al.* Cytokinocytes: the diverse contribution of keratinocytes to immune responses in skin. *JCI Insight* **5**, e142067.

48. Piipponen, M., Li, D. & Landén, N. X. The Immune Functions of Keratinocytes in Skin Wound Healing. *Int. J. Mol. Sci.* **21**, 8790 (2020).

49. Clayton, K., Vallejo, A. F., Davies, J., Sirvent, S. & Polak, M. E. Langerhans Cells—Programmed by the Epidermis. *Front. Immunol.* **8**, 1676 (2017).

50. Ross, E. A., Devitt, A. & Johnson, J. R. Macrophages: The Good, the Bad, and the Gluttony. *Front. Immunol.* **12**, (2021).

51. Krystel-Whittemore, M., Dileepan, K. N. & Wood, J. G. Mast Cell: A Multi-Functional Master Cell. *Front. Immunol.* **6**, (2016).

52. Serbina, N. V., Jia, T., Hohl, T. M. & Pamer, E. G. Monocyte-Mediated Defense Against Microbial Pathogens. *Annu. Rev. Immunol.* **26**, 421–452 (2008).

53. Selders, G. S., Fetz, A. E., Radic, M. Z. & Bowlin, G. L. An overview of the role of neutrophils in innate immunity, inflammation and host-biomaterial integration. *Regen. Biomater.* **4**, 55–68 (2017).

54. Abel, A. M., Yang, C., Thakar, M. S. & Malarkannan, S. Natural Killer Cells: Development, Maturation, and Clinical Utilization. *Front. Immunol.* **9**, (2018).

55. Björkström, N. K., Strunz, B. & Ljunggren, H.-G. Natural killer cells in antiviral immunity. *Nat. Rev. Immunol.* **22**, 112–123 (2022).

56. Charles A Janeway, J., Travers, P., Walport, M. & Shlomchik, M. J. B-cell activation by armed helper T cells. in *Immunobiology: The Immune System in Health and Disease. 5th edition* (Garland Science, 2001).
57. Puniya, B. L. *et al.* A Mechanistic Computational Model Reveals That Plasticity of CD4+ T Cell Differentiation Is a Function of Cytokine Composition and Dosage. *Front. Physiol.* **9**, 878 (2018).
58. Zhu, J., Yamane, H. & Paul, W. E. Differentiation of Effector CD4 T Cell Populations. *Annu. Rev. Immunol.* **28**, 445–489 (2010).
59. CD4+T Cells: Differentiation and Functions. https://www.hindawi.com/journals/jir/2012/925135/.
60. Harrington, L. E. *et al.* Interleukin 17–producing CD4 + effector T cells develop via a lineage distinct from the T helper type 1 and 2 lineages. *Nat. Immunol.* **6**, 1123–1132 (2005).
61. Charles A Janeway, J., Travers, P., Walport, M. & Shlomchik, M. J. T cell-mediated cytotoxicity. in *Immunobiology: The Immune System in Health and Disease. 5th edition* (Garland Science, 2001).
62. Zhang, N. & Bevan, M. J. CD8+ T Cells: Foot Soldiers of the Immune System. *Immunity* **35**, 161–168 (2011).
63. Vivier, E., Ugolini, S., Blaise, D., Chabannon, C. & Brossay, L. Targeting natural killer cells and natural killer T cells in cancer. *Nat. Rev. Immunol.* **12**, 239–252 (2012).
64. Bucşan, A. N. & Williamson, K. C. Setting the stage: The initial immune response to blood-stage parasites. *Virulence* **11**, 88–103 (2020).
65. Stevenson, M. M. & Riley, E. M. Innate immunity to malaria. *Nat. Rev. Immunol.* **4**, 169–180 (2004).
66. Stanley, M. Immune responses to human papillomavirus. *Vaccine* **24 Suppl 1**, S16-22 (2006).
67. Olukitibi, T. A., Ao, Z., Mahmoudi, M., Kobinger, G. A. & Yao, X. Dendritic

Cells/Macrophages-Targeting Feature of Ebola Glycoprotein and its Potential as Immunological Facilitator for Antiviral Vaccine Approach. *Microorganisms* **7**, 402 (2019).

68. Zhai, W., Wu, F., Zhang, Y., Fu, Y. & Liu, Z. The Immune Escape Mechanisms of Mycobacterium Tuberculosis. *Int. J. Mol. Sci.* **20**, 340 (2019).
69. Caccamo, N. *et al.* Human CD8 T lymphocytes recognize Mycobacterium tuberculosis antigens presented by HLA-E during active tuberculosis and express type 2 cytokines. *Eur. J. Immunol.* **45**, 1069–1081 (2015).
70. Carrington, M. & Alter, G. Innate Immune Control of HIV. *Cold Spring Harb. Perspect. Med.* **2**, a007070 (2012).
71. Motran, C. C. *et al.* Helminth Infections: Recognition and Modulation of the Immune Response by Innate Immune Cells. *Front. Immunol.* **9**, (2018).
72. Awasthi, A., Mathur, R. K. & Saha, B. Immune response to Leishmania infection. *Indian J. Med. Res.* **119**, 238–258 (2004).
73. Chen, X. *et al.* Host Immune Response to Influenza A Virus Infection. *Front. Immunol.* **9**, 320 (2018).
74. Richardson, J. P. & Moyes, D. L. Adaptive immune responses to Candida albicans infection. *Virulence* **6**, 327–337 (2015).
75. Babu, S. & Nutman, T. B. 31 - Immune Responses to Helminth Infection. in *Clinical Immunology (Fifth Edition)* (eds. Rich, R. R. et al.) 437-447.e1 (Elsevier, 2019). doi:10.1016/B978-0-7020-6896-6.00031-4.
76. Banks, H. T., Davidian, M., Hu, S., Kepler, G. M. & Rosenberg, E. S. Modelling HIV immune response and validation with clinical data. *J. Biol. Dyn.* **2**, 357–385 (2008).
77. Scott, M., Nakagawa, M. & Moscicki, A.-B. Cell-Mediated Immune Response to Human Papillomavirus Infection. *Clin. Diagn. Lab. Immunol.* **8**, 209–220 (2001).
78. Leroy, E. M., Baize, S., Debre, P., Lansoud-Soukate, J. & Mavoungou, E. Early immune responses accompanying human asymptomatic Ebola infections. *Clin. Exp. Immunol.* **124**,

453–460 (2001).

79. Ada, G. L. & Jones, P. D. The Immune Response to Influenza Infection. in *Current Topics in Microbiology and Immunology* (eds. Clarke, A. et al.) 1–54 (Springer, 1986). doi:10.1007/978-3-642-71272-2_1.
80. O'Garra, A. *et al.* The immune response in tuberculosis. *Annu. Rev. Immunol.* **31**, 475–527 (2013).
81. Gause, W. C., Wynn, T. A. & Allen, J. E. Type 2 immunity and wound healing: evolutionary refinement of adaptive immunity by helminths. *Nat. Rev. Immunol.* **13**, 607–614 (2013).
82. Wenisch, C., Parschalk, B., Narzt, E., Looareesuwan, S. & Graninger, W. Elevated serum levels of IL-10 and IFN-gamma in patients with acute Plasmodium falciparum malaria. *Clin. Immunol. Immunopathol.* **74**, 115–117 (1995).
83. Brustoski, K. *et al.* IFN-gamma and IL-10 mediate parasite-specific immune responses of cord blood cells induced by pregnancy-associated Plasmodium falciparum malaria. *J. Immunol. Baltim. Md 1950* **174**, 1738–1745 (2005).
84. Qin, Y. *et al.* Innate immune cell response upon Candida albicans infection. *Virulence* **7**, 512–526 (2016).
85. Reynard, S. *et al.* Immune parameters and outcomes during Ebola virus disease. *JCI Insight* **4**, e125106 (2019).
86. Berti, F. C. B., Pereira, A. P. L., Cebinelli, G. C. M., Trugilo, K. P. & Brajão de Oliveira, K. The role of interleukin 10 in human papilloma virus infection and progression to cervical carcinoma. *Cytokine Growth Factor Rev.* **34**, 1–13 (2017).
87. Cooper, P. J. *et al.* Human infection with Ascaris lumbricoides is associated with a polarized cytokine response. *J. Infect. Dis.* **182**, 1207–1213 (2000).
88. Tavares, L. P., Teixeira, M. M. & Garcia, C. C. The inflammatory response triggered by Influenza virus: a two edged sword. *Inflamm. Res. Off. J. Eur. Histamine Res. Soc. Al* **66**, 283–302 (2017).

89. Frimpong, A. *et al.* Asymptomatic Malaria Infection Is Maintained by a Balanced Pro- and Anti-inflammatory Response. *Front. Microbiol.* **11**, 559255 (2020).
90. Domingo-Gonzalez, R., Prince, O., Cooper, A. & Khader, S. A. Cytokines and Chemokines in Mycobacterium tuberculosis Infection. *Microbiol. Spectr.* **4**, (2016).
91. Torres-Poveda, K. *et al.* Role of IL-10 and TGF-β1 in local immunosuppression in HPV-associated cervical neoplasia. *World J. Clin. Oncol.* **5**, 753–763 (2014).
92. Flynn, J. L. *et al.* An essential role for interferon gamma in resistance to Mycobacterium tuberculosis infection. *J. Exp. Med.* **178**, 2249–2254 (1993).
93. Wertheim, K. Y. *et al.* A multi-approach and multi-scale platform to model CD4+ T cells responding to infections. *PLOS Comput. Biol.* **17**, e1009209 (2021).
94. Raza, S. *et al.* A logic-based diagram of signalling pathways central to macrophage activation. *BMC Syst. Biol.* **2**, 36 (2008).
95. Puniya, B. L. *et al.* Integrative computational approach identifies drug targets in CD4+ T-cell-mediated immune disorders. *Npj Syst. Biol. Appl.* **7**, 1–18 (2021).
96. Wagner, A. *et al.* Metabolic Modeling of Single Th17 Cells Reveals Regulators of Autoimmunity. *Cell* **184**, 4168-4185.e21 (2021).
97. Bordbar, A. *et al.* Model-driven multi-omic data analysis elucidates metabolic immunomodulators of macrophage activation. *Mol. Syst. Biol.* **8**, 558 (2012).